Local Conformation of Regular Star Polymers in a Good Solvent: A Monte Carlo Study

Alessandra Forni,[†] Fabio Ganazzoli,*,[†] and Michele Vacatello[‡]

Dipartimento di Chimica, Politecnico di Milano, via L. Mancinelli 7, I-20131 Milano, Italy, and Dipartimento di Chimica, Università di Napoli, via Mezzocannone 4, I-80134 Napoli, Italy

Received June 22, 1995; Revised Manuscript Received October 20, 1995[⊗]

ABSTRACT: Off-lattice Monte Carlo simulations were performed on linear and 12-arm regular star polymers with up to 472 repeat units in the excluded-volume regime. For both topologies, the overall size scales asymptotically with molecular weight through a Flory exponent, $\nu = 0.588$, but for finite molecular weights, the apparent exponent is slightly different in the case of the radius of gyration and of the root-mean-square end-to-end distance and definitely smaller in the case of the hydrodynamic radius. The interatomic distances within the star follow a 2-fold behavior, according to whether the two atoms belong to the same arm or to different arms. This result is related with the peculiar behavior of the scalar products among the bond vectors. If these belong to the same arm and are remote from the branch point, the scalar products follow the same pattern as in the linear chain. If however the bonds are close to the branch point, the scalar products are much larger and essentially constant, indicating a substantial arm stretching. Conversely, if the two bonds are on different arms, the scalar products across the branch point drop at once by more than 1 order of magnitude. Therefore, the initial arm directions are essentially noncorrelated, and the interarm repulsions are best accommodated with a minimum entropy loss.

Introduction

The conformation of regular star polymers is a topic of interest both in itself and from a theoretical viewpoint as a check of the intramolecular interactions within branched polymers.[1] The configurational normal-mode description of polymers in a good solvent with self-consistent free-energy minimization[2] was recently applied to regular stars in ref 3, hereafter denoted as paper I. The N normal modes are simple linear combinations of the N chain bond vectors in a coarse-grained description; in this way, all the relevant conformational degrees of freedom are accounted for through the strain ratios of the mean-square amplitudes of the normal modes that form the unknowns of the problem. This procedure rests on the assumption of a Gaussian distribution for the interatomic distances and, furthermore, requires a prior knowledge of the normal modes. In the absence of intramolecular interactions, these can be determined from the symmetry of the star polymer; however, under excluded-volume expansion, these "normal" modes are no more orthogonal, strictly speaking, due to the long-range interactions. Therefore, the procedure was modified to account for the possible cross terms among normal modes of the same parity with respect to the branch point.[3] Still assuming a Gaussian distribution, it was shown in paper I that this nonorthogonality can be neglected to a very good approximation provided the degree of expansion is not too large in 6-arm star polymers and, *a fortiori*, linear chains. Concerning the star conformation, the bond vectors across the branch point display a strong loss of correlation, so that the chain expansion is mostly concentrated in the central region of the star *within each arm*. In this way, the polymer may best accommodate the interatomic repulsions without excessive overcrowding among the different arms. This loss of correlation is also evident in the pattern of the interatomic distances, $\langle r^2_{ij}\rangle$ (Figure 2 of paper I): Plots of $\langle r^2_{ij}\rangle$ for a fixed i show a finite discontinuity in the first derivative when j passes across the branch point. These results rely only on the Gaussian approximation, which is known to be incorrect in principle under good-solvent expansion. However, because of the very existence of the branch point, it is difficult to abandon such an approximation in the star, as shown, for example, by the lengthy renormalization group results of Miyake and Freed.[4] Moreover, only the Gaussian approximation allows us to use linear equations when dealing with polymer dynamics to express the elastic force acting on each chain atom.[2,5]

In order to test this approximation and the equilibrium results above mentioned, we resorted to Monte Carlo simulations that do not assume any *a priori* distribution function. Extensive simulation results do already exist in the literature (see, e.g., refs 6−14 and citations therein) but are mostly concerned with overall properties such as the radius of gyration either in the Θ state or in a good solvent. Some results about local properties were also reported[6,8] but do not deal with the specific effect discussed above or lead to somewhat inconclusive results as far as the bond-vector correlation is concerned (see later). In the next sections, after a description of the simulation method, we first report our results for the overall molecular size, as a check of the excluded-volume regime, and then we turn to the local properties. In this case, many results will also be summarized through simple power laws. The corresponding exponents, however, are not universal and can be used only for a comparison of the star with the linear chain.

Monte Carlo Simulation

The polymers were modeled as connected chains of identical beads (atoms), with a unit length of the links (bonds) between consecutive beads. Beads separated by two or more bonds interact through a 6−12 Lennard−Jones potential with mini-

---

[†] Politecnico di Milano.

[‡] Università di Napoli.

[⊗] Abstract published in *Advance ACS Abstracts*, March 1, 1996.

Chart 1

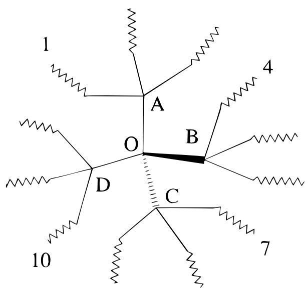

mum energy at a distance equal to the bond length, i.e.,

$$E(r_{ij}) = \epsilon\left(\frac{1}{r_{ij}^{12}} - \frac{2}{r_{ij}^{6}}\right) \qquad (1)$$

with an energy parameter of $\epsilon/k_BT = 0.05$. We considered star polymers with $f = 12$ arms, having the structure shown in Chart 1: Four bonds depart from the central branch point O with a fixed tetrahedral geometry, and three arms follow from each secondary branch point (A−D) with no further geometrical constraint. With this structure, the total number of bonds, N, and the arm length, n, are related by $N = nf - 8$. We generated star polymers with arm lengths up to $n = 40$, hence $N = 472$, and linear chains with the same N values, using the same structure just described, in particular with the same fixed tetrahedral geometry at the central atom. Therefore, the linear chains have $N = nf$.

Off-lattice Monte Carlo simulations were performed starting from an initial conformation with the bonds connected to the secondary branch points in a staggered conformation with respect to the central tetrahedron and the subsequent bonds in a completely extended conformation (bond angles of 180°). Then we let this conformation equilibrate before computing the averages of interest. At each step one bead was randomly selected, and the smaller of the two polymer portions connected to it was rigidly rotated at random around a random axis through the selected bead (only the central five atoms of the star, or three atoms for the linear chain, were kept fixed during all the simulations). The equilibration and the sampling of the equilibrium conformations were realized according to the standard Metropolis algorithm.[15,16]

We first checked that the chosen energy parameter was appropriate for good-solvent conditions by first calculating the molecular weight dependence of the molecular size, i.e., the mean-square end-to-end distance, $\langle R^2\rangle$ (in the star this is taken as the average value over all the possible free ends), the mean-square radius of gyration, $\langle S^2\rangle$, and the hydrodynamic radius, R_H. The latter is *defined* as

$$R_H^{-1} = (N+1)^{-2}\sum_{i<j}\langle r_{ij}^{-1}\rangle \qquad (2)$$

and coincides with the experimental quantity obtained from the measurement of the diffusion coefficient only within the Kirkwood−Riseman approximation in the large molecular weight limit.[2,17] Then we investigated local properties such as the mean-square interatomic distances, $\langle r^2_{ij}\rangle$, and the correlation among bond vectors through their average scalar products, $\langle \mathbf{l}_i\cdot\mathbf{l}_j\rangle$. In the star, if i and j belong to the same arm, we consider the distances $\langle r^2_{ij}\rangle$ within one arm only. Since however no complete equivalence is found between different pairs of arms, in general, unless after a huge number of Monte Carlo steps (see also later), the interarm $\langle r^2_{ij}\rangle$ values are then further averaged over three topologically equivalent distances, where i is kept on arm 1, and j is in turn on arms 4, 7, and 10 (see Chart 1). The same four arms were considered for the scalar products $\langle \mathbf{l}_i\cdot\mathbf{l}_j\rangle$, the averages being taken over *all* the possible intra- and interarm scalar products among the topologically equivalent bond vectors. This procedure was also followed for the linear chains, where only two "arms" are obviously present.

For a given polymer, we calculated all the average properties starting from the same "equilibrium" conformation that is attained from the initial conformation through a number, m, of successful Monte Carlo transitions (or steps, for short) which depend both on the total number of bonds and on the polymer topology. Though in general no rigorous relationship exists between the successive conformations and the real time evolution of the system, we may assume that the scaling law for the longest relaxation time, τ_1, in the Rouse limit [$\tau_1 \propto (N/f)^2$] provides an estimate of the Monte Carlo relaxation "time" (i.e., number of steps) required to equilibrate stars ($f = 12$ in our case) in comparison with linear chains ($f = 2$). In this way, using for both polymers the equilibration "time" of the linear chain with the same N, spurious effects due to a lack of complete equilibration of the star were avoided.

In order to determine the number m of Monte Carlo steps required to equilibrate the linear chain, we inspected the variation of the scalar products $\mathbf{l}_i\cdot\mathbf{l}_j$ among the bond vectors. This is the slowest relaxing property, since its instantaneous value does not involve any implicit averaging over the chain conformation. In fact, the instantaneous S^2 may be viewed as an "average" over the interatomic distances r^2_{ij} and these, in turn, as suitable "averages" over the scalar products $\mathbf{l}_i\cdot\mathbf{l}_j$. As an example, for the largest chain considered in our simulations ($N = 472$ bonds), the overall properties reached the equilibrium value in a few hundred steps, whereas we had to wait for up to $m = 5 \times 10^5$ steps for the equilibration of the local properties. The subsequent calculation of the average properties was performed with a number of Monte Carlo steps equal to or larger than that required for the equilibration. For instance, the scalar products were evaluated with $m = 2 \times 10^6$ steps. The number of trials required to perform a given number of successful transitions weakly increased with N, but it also depended on the chain topology, being somewhat larger for the star. More than 40% of the Monte Carlo trials were, anyway, successful in all our calculations. To improve the statistical accuracy of the scalar products $\langle \mathbf{l}_i\cdot\mathbf{l}_j\rangle$, we further averaged the results over three independent runs, although none of them was appreciably different from the average behavior (see the corresponding section in the following). Typical error bars for $\langle \mathbf{l}_i\cdot\mathbf{l}_j\rangle$ are shown in Figure 4, whereas they are smaller than the symbol size for $\langle R^2\rangle$, $\langle S^2\rangle$, R_H, and $\langle r^2_{ij}\rangle$ in Figures 1−3. Also, we can roughly estimate the error in the exponents of the power laws reported in the text as ±1 in the last digit.

Results and Discussion

Overall Properties. We first investigated the molecular weight dependence of the overall properties to check that the polymers are indeed in the full excluded-volume regime. In particular, we look for a power-law relationship with a critical Flory exponent, ν, close to the value 0.588 predicted by LeGuillou and Zinn-Justin.[18] In Figure 1 we report the mean-square radius of gyration, $\langle S^2\rangle$, the mean-square end-to-end distance, $\langle R^2\rangle$, and the "hydrodynamic" radius, R_H (from eq 2), as a function of the total number of bonds N. The appropriate Flory exponents are

$$\begin{aligned}\langle S^2\rangle &\propto N^{2\nu_S} \quad \nu_S^{\ \mathrm{lin}} = 0.597 \quad \nu_S^{\ \mathrm{star}} = 0.573\\ \langle R^2\rangle &\propto N^{2\nu_R} \quad \nu_R^{\ \mathrm{lin}} = 0.595 \quad \nu_R^{\ \mathrm{star}} = 0.592 \qquad (3)\\ R_H &\propto N^{\nu_H} \quad \nu_H^{\ \mathrm{lin}} = 0.514 \quad \nu_H^{\ \mathrm{star}} = 0.515\end{aligned}$$

Although the range of N (≤472) is not large enough to have accurate values of the exponents, and moreover the number of points is quite limited, nonetheless we see that for the linear chain $\nu_R \cong \nu_S$, whereas for the star we find $\nu_R > \nu_S$ (see also refs 6 and 13). Moreover, the ν_H exponents are much smaller that the other ones, in qualitative agreement with published results.[6,17]

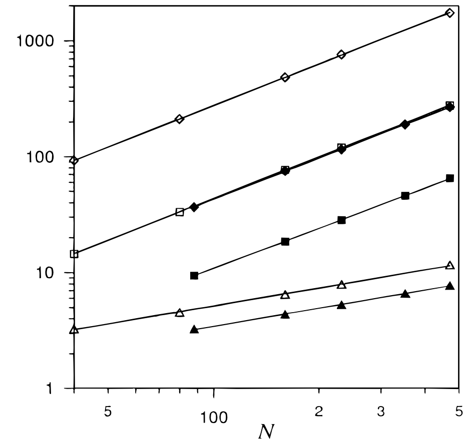

Figure 1. Mean-square radii of gyration, $\langle S^2\rangle$, mean-square end-to-end distance, $\langle R^2\rangle$, and hydrodynamic radius, R_H (from eq 2), as a function of the total number of bonds, N. The filled symbols indicate the star and the empty symbols the linear chain. The squares indicate $\langle S^2\rangle$, the diamonds $\langle R^2\rangle$, and the triangles R_H (note that $\langle R^2\rangle_{star}$ and $\langle S^2\rangle_{lin}$ accidentally coincide). The straight lines are the least-squares fits yielding the exponents of eq 3.

Although not clearly evident from inspection of Figure 1, all these exponents are still changing somewhat with N, in particular ν_H: For example, a fit over the few values obtained with $N > 200$ yields $\nu_H \cong 0.54$ for both topologies. Interestingly, Batoulis and Kremer[6] simulated linear and star polymers with $f \leq 6$ on a face-centered cubic lattice with $N \leq 400$ and found the same molecular weight dependence for ν_R and ν_H but not for ν_S, which was equal to 0.588 throughout. Still, our results are consistent with a common asymptotic exponent of $\nu = 0.588$. In keeping with the suggestion of Batoulis and Kremer,[6] we plotted our results as $\langle S^2\rangle/N^{2\nu}$, $\langle R^2\rangle/N^{2\nu}$ or R_H/N^{ν}, vs $N^{-1/2}$ with $\nu = 0.588$. In all cases we obtained straight lines, suggesting that this is also our asymptotic, universal exponent and showing that we are indeed in the full excluded-volume regime. Therefore, the exponents of eq 3 are due to the finiteness of the chain, which is more important for R_H, since it is given by the sum of the reciprocal interatomic distances[6,17,19] and the asymptotic exponent would be attained only at extremely large molecular weights. It must also be pointed out that experimentally one determines precisely an "apparent" exponent, with values generally close to those reported here.[17,20,21]

As a further check, we also calculated the topological ratios $g_S = \langle S^2\rangle_{star}/\langle S^2\rangle_{lin}$ and $g_H = R_{H,star}/R_{H,lin}$ from the results of Figure 1. We get $g_S \cong 0.235$ and $g_H = 0.667$ for the larger molecular weights; the asymptotic values, obtained upon the extrapolation of $\langle S^2\rangle/N^{2\nu}$ and R_H/N^{ν} for $N^{-1/2} \rightarrow 0$ discussed before, are $g_S \cong 0.222$ and $g_H \cong 0.656$. g_S is therefore almost equal to the phantom chain value[22] 0.236 [$g_S{}^{ph} = (3f - 2)/f^2$], in agreement with previous results (see refs 1 and 3 and citations therein). Conversely, g_H is larger than the phantom chain value[23] 0.623 [$g_H{}^{ph} = f^{1/2}/(2 - f + \sqrt{2}(f - 1))$] but is still somewhat smaller than the experimental values[1] that suggest $g_H \geq 0.70$ for 12-arm stars. The approximations about the chain dynamics implicit in eq 2 are well known, concerning in particular the use of the preaveraged hydrodynamic interaction (see ref 1 for a clear and concise review), and therefore comparison with experiment is not fully significant.

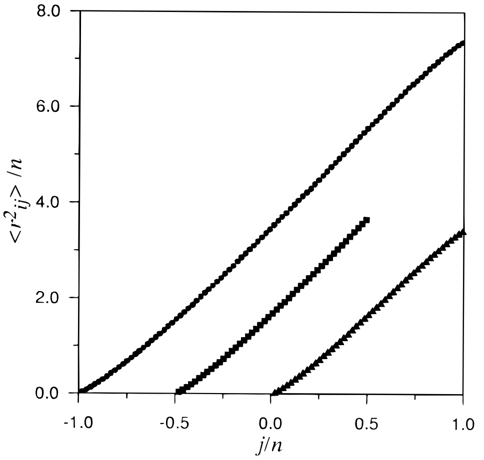

Figure 2. Normalized interatomic distances, $\langle r^2{}_{ij}\rangle/n$, plotted as a function of j/n for the linear chain with $N = 472$ total bonds and $n = 236$ bonds/arm. The atoms are labeled as negative from $-n$ to 0 (the central atom) on the first arm and as positive up to n on the second arm. Three different locations of the first atom i are $i = -n$, i.e., at one free end (●); $i = -n/2$, i.e., at the midpoint of the first arm (■); and $i = 0$, i.e., at the central atom of the whole chain (▲). Only one point in every five is reported for clarity.

Local Properties: Interatomic Distances. Let us turn now to the local properties that form the main purpose of the present work. Figures 2 and 3 show the mean-square interatomic distances, $\langle r^2{}_{ij}\rangle$, for fixed i's plotted as a function of j for linear and star polymers with 472 total bonds, or 40 bonds/arm in the star. Three curves are reported in each figure, corresponding to three different positions of the fixed atom i. In the first curve i sits at one free end with j running to the other free end, in the second curve i is at the midpoint of an arm while j runs until the midpoint of the second arm, and in the third curve i is the central atom and j runs to the free end. In the linear polymer, the distances increase smoothly with the topological separation, $|j - i|$ (see Figure 2), whereas the analogous plots for the star are qualitatively different, as shown in Figure 3. The difference with the linear chain is most evident when j crosses the central branch point and the curves show a cusp point, with a finite discontinuity in the first derivatives. This is a general feature of the star, irrespective of molecular weight or the location of i. (Note that the cusp point is *not* related with the fixed tetrahedral bond angle at the central atom, since this constraint does not affect in any way the linear chain plot; see Figure 2.) As discussed in paper I, the very existence of this cusp point is indicative of an abrupt loss of correlation among the arms, related with their mutual steric interference. We discuss this effect in the next section through the scalar products among the bond vectors.

In connection with the star plots of Figure 3, it is worth recalling that the mean-square distances, $\langle r^2{}_{ij}\rangle$, between atoms i and j located on different arms are computed as averages of three values obtained by choosing i on arm 1 and j on arms 4, 7, and 10 (see Chart 1). The mean-square distances corresponding to the three choices differ systematically among themselves by about 5% (the curves are not reported in Figure 3 for clarity), one of the latter three arms being on the average closer to arm 1. By resuming the simulation for an equal number of Monte Carlo steps, the three arms scramble their relative position, without any significant difference in the average plot. This observation suggests that the time needed for the complete relaxation within each arm, though much longer than the relaxation time of the radius of gyration, still is

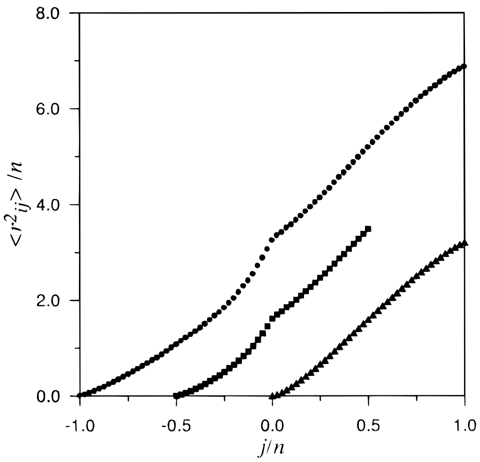

Figure 3. Same as in Figure 2 for the star. The three locations of the first atom i correspond to $i = -n$, i.e., at one free end (●); $i = -n/2$, at the midpoint of the first arm (■); and $i = 0$, i.e., at the central branch point (▲).

much shorter than the time required by the arms to lose memory of their relative positions because of the inter-arm hindrance (here, of course, "time" loosely means "number of Monte Carlo steps"). We checked that this memory effect is enhanced by an increasing arm length, whereas it is almost absent for very short arms. This finding is possibly related with the observation that linear and star polymers[11,24] are characterized by a fluctuating ellipsoidal shape, although tending on the average to a spherical symmetry. By analyzing the eigenvalues of the radius-of-gyration tensor[24] of 3- and 4-arm stars, Su et al.[11] found that the asphericity of stars decreases with the number of arms, so we expect that it is very small for 12-arm stars, but still it makes some arms to be closer on the average, as observed by us.

In general, $\langle r^2_{ij}\rangle$ depends on the location of the two atoms within the chain. However, at least for the linear chain, if both atoms are far from the chain ends, we may expect that $\langle r^2_{ij}\rangle$ depends only on the topological separation, $|j - i|$. Therefore, in analogy with eq 3, we looked for a power law of the general form

$$\langle r^2_{ij}\rangle \propto |j - i|^{2\nu_{ij}} \tag{4}$$

where the exponent may still depend on the position of the two atoms. For the linear chain (from Figure 2, $N = 472$), we get

$$\nu_{ij}^{\text{lin}} = 0.597 \tag{5$'$}$$

if i is at one free end and j spans the whole chain, and

$$\nu_{ij}^{\text{lin}} = 0.605 \tag{5$''$}$$

if i is at the midpoint of one arm ($^1/_4$ of the chain length) and j spans the central half. In the former case ν_{ij}^{lin} is identical with ν_R^{lin} and ν_S^{lin}, whereas in the latter case ν_{ij}^{lin} is slightly larger, in keeping with the idea that the expansion is larger in the central section of the chain because of the outer portions. It should be kept in mind however that these exponents are still affected by the chain length (see also later) and have no universal meaning but are useful for a comparison with the star in the following.

No simple power law can hold for the star if the second atom moves *across* the branch point. Even within one arm, the location of both i and j is more important than in the linear chain; nevertheless, by forcing the power law of eq 4 to this case, we get

$$\nu_{ij}^{\text{star}} = 0.645 \tag{6$'$}$$

if i is at one free end, and

$$\nu_{ij}^{\text{star}} = 0.682 \tag{6$''$}$$

if i is at the midpoint of one arm, while j moves up to the central branch point in either case. These exponents are significantly larger than in linear chains, even if these had the same arm length. If i is at one free end and j spans the whole chain, we find, for instance, $\nu_{ij}^{\text{lin}} = 0.634$ (40 total bonds) or 0.626 (80 total bonds). The larger exponents of the star indicate a significantly greater expansion, due to the repulsive interactions among the arms. This expansion is concentrated in the core region, where the local density is larger, as shown by the strong uprise of the curves of $\langle r^2_{ij}\rangle$ when the second atom is close to the branch point (see Figure 3). It is precisely this uprise that makes the exponent larger in eq 6″ than that in eq 6′ because the atoms near the branch point have a larger weight. At the same time, it suggests that the power-law relationship in eq 4 is not adequate for finite arm lengths. If the two atoms are far from both the free ends and the branch point, we cannot rule out the possibility that the ν_{ij} exponents of the two topologies are asymptotically equal, although the very existence of the cusp point in the star is a further manifestation of an architecture intrinsically different from the linear one.

Local Properties: Bond-Vector Correlation. Both the large expansion close to the branch point within each arm and the loss of correlation among the arms displayed by the star are best evident in the behavior of the scalar products $\langle \mathbf{l}_i\cdot\mathbf{l}_j\rangle$ among the bond vectors. In the following we adopt throughout the convention of a head-to-tail connection of the bond vectors. In this way, positive values of the scalar products indicate an expansion with respect to the random walk (where $\langle \mathbf{l}_i\cdot\mathbf{l}_j\rangle = \delta_{ij}$), whereas negative values are indicative of contraction. Plots of $\langle \mathbf{l}_i\cdot\mathbf{l}_j\rangle$ are reported in Figures 4 and 5 as a function of $|j - i|$ for a fixed position of the first bond $\mathbf{l}_i$. Figure 4 shows $\langle \mathbf{l}_i\cdot\mathbf{l}_j\rangle$ for the star (empty squares; $n = 40$ and $N = 472$), when $\mathbf{l}_i$ is far from the branch point and $\mathbf{l}_j$ approaches the free end. For comparison, we also show $\langle \mathbf{l}_i\cdot\mathbf{l}_j\rangle$ for two linear chains. The first chain has the same number of total bonds (filled squares; $N = 472$), with $\mathbf{l}_i$ located in proximity of the center of an arm, although the pattern is insensitive to its exact location provided both bonds are far from the free ends. The second chain has the same number of bonds per arm (filled triangles; $n = 40$, hence $N = 80$), and $\mathbf{l}_i$ is in the same position as in the star. In all cases the bond $\mathbf{l}_j$ approaches the closer free end. The three curves of Figure 4 are quite similar, with $\langle \mathbf{l}_i\cdot\mathbf{l}_j\rangle$ smoothly decreasing with the topological separation, $|j-i|$, but some differences are evident, although close to the limit of the statistical significance. In the largest linear polymer (filled squares), the end effects are negligible and the scalar products depend only on the topological separation, $|j-i|$, unlike in the shorter linear polymer (filled triangles), where for $|j - i| > 10$ a loss of correlation begins to appear due to the proximity of the free end (here and in the star $\mathbf{l}_j$ runs up to the fifth bond from the end). In fact, the end bonds have little correlation

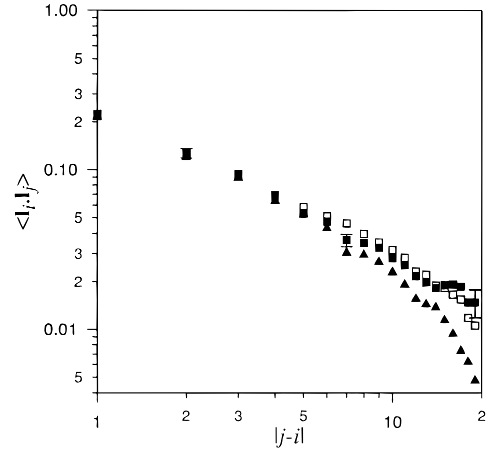

Figure 4. Scalar products, $\langle \mathbf{l}_i \cdot \mathbf{l}_j \rangle$, plotted as a function of the topological separation, $|j - i|$. In all cases the position of the first bond $\mathbf{l}_i$ is kept fixed, while $\mathbf{l}_j$ approaches the closest free end. The bonds are numbered starting from the central branch point: (■) the linear chain with $N = 472$ total bonds and $\mathbf{l}_i$ is near the central bond of an arm ($i = 99$), (□) the star with $N = 472$ total bonds and $n = 40$ bonds/arm, with $i = 17$, and (▲) the linear chain with $N = 80$ total bonds, hence $n = 40$ bonds/arm, with $i = 17$ (note that in the last two cases $\mathbf{l}_j$ arrives at a 4-bond distance from the free end). The estimated standard deviations for the three polymers are equal, at a given topological separation; some typical values are shown for the longer linear chain at $|j - i| = 2$, 7, and 19.

with the inner bonds for entropic reasons. In the star (empty squares) this effect is less pronounced because of the greater arm expansion.

In the central parts of the arms, where we may expect that only the topological separation matters, we looked for the power law

$$\langle \mathbf{l}_i \cdot \mathbf{l}_j \rangle \propto |j - i|^{-\mu} \qquad (7)$$

in analogy to what was done above. μ must be smaller than 1; otherwise we would asymptotically have $\langle S^2 \rangle \propto \langle R^2 \rangle \propto N$, as in the unperturbed state. In fact, it may be shown that the relationship $\mu = 2 - 2\nu$ must eventually hold, at least for large $|j - i|$, in order to account for eqs 3 and 4. A reliable estimate of μ is somewhat difficult because of the relatively limited range of bond separation that we can analyze while keeping both bonds remote from the chain ends or the branch point, and therefore μ is even farther from a universal exponent than ν_{ij} in eqs 5 and 6. Moreover, a very large statistical accuracy is required to the simulation because of the small values of the scalar products for large $|j - i|$. Nevertheless, considering the largest linear chain, where the finite-size effects should be smaller, the average value of μ, obtained for different positions of the fixed bond $\mathbf{l}_i$, turns out to be about 0.95. In the star, discarding the bonds close to the free end (i.e., values $|j - i| > 10$), we obtain $\mu = 0.82$, considerably smaller than the value for the linear chain. This difference reflects the larger expansion of the star and is consistent with its larger values of the ν_{ij} exponent (compare eq 6 with eq 5). On the other hand, the fit carried out on the same range of $|j - i|$ for the linear chain with the same arm length ($n = 40$) yields $\mu = 0.99$, indicating that the effect of the free end is stronger and causes the chain to approach somewhat the random-walk regime. (Incidentally, note that $\mu = 1$ implies logarithmic corrections to the interatomic distances.) The larger correlation among the bond vectors within one arm of the star compared to the linear chain is in qualitative agreement with previous Monte Carlo simulations.[6,25]

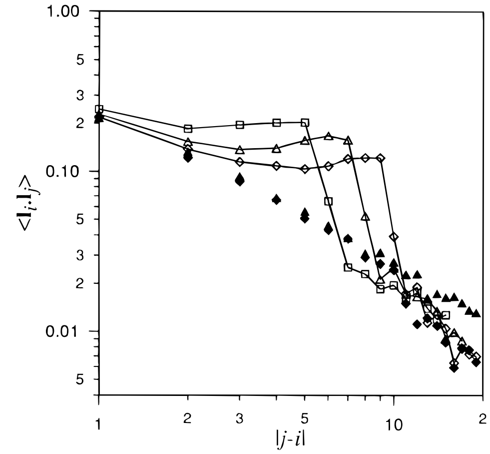

Figure 5. Scalar products, $\langle \mathbf{l}_i \cdot \mathbf{l}_j \rangle$, plotted as a function of the topological separation, $|j - i|$. In all cases the position of the first bond $\mathbf{l}_i$ is kept fixed, while $\mathbf{l}_j$ crosses the central branch point (or the central atom in the linear chain). The bonds are numbered starting from the free end: (◆) the linear chain with $N = 40$ total bonds and $n = 20$ bonds/arm, with $i = 11$ (the central atom is connected to bonds 20 and 21), (▲) the linear chain with $N = 80$ and $n = 40$, with $i = 31$ (the central atom is connected to bonds 40 and 41). The empty symbols, connected by a solid line for clarity, show three different choices for the position of $\mathbf{l}_i$ in the star with $N = 232$ total bonds and $n = 20$ bonds/arm (the central branch point is comprised between bonds 20 and 21), (◇) $i = 11$ (the branch point is reached after $j - i = 9$ bonds), (△) $i = 13$ (the branch point is reached after $j - i = 7$ bonds), and (□) $i = 15$ (the branch point is reached after $j - i = 5$ bonds). Therefore, the sudden drops of the scalar products always take place when $\mathbf{l}_j$ goes across the central branch point into the second arm (see text and Chart 1).

In Figure 5 we report the scalar products $\langle \mathbf{l}_i \cdot \mathbf{l}_j \rangle$ with $\mathbf{l}_i$ and $\mathbf{l}_j$ close to the branch point for the star (empty symbols) and close to the chain midpoint for the linear polymers (filled symbols). We show results for linear chains with $n = 20$ and 40 bonds/arm and for the star with $n = 20$ ($N = 232$ total bonds). Three different positions of the starting bond $\mathbf{l}_i$ are shown for the star, to stress the different behavior from the linear chain. In all cases, $\mathbf{l}_j$ runs toward the central branch point and then away from it when on the second arm. The difference between the linear chain and the star is striking. For the linear chain we obviously observe the same behavior discussed above (note incidentally that the fixed tetrahedral angle at the central atom does not affect the plot; see Figures 4 and 5, filled symbols). On the other hand, the star shows a 2-fold behavior. If $\mathbf{l}_j$ is still on the same arm as $\mathbf{l}_i$, the scalar products are much larger than in the linear polymer and, indeed, are essentially constant and independent from the topological separation, as denoted by the strong similarity of the three curves of the star. This large and constant correlation when both bonds are on the same arm in the close vicinity of the star core corresponds to the larger expansion of the star arm compared to the linear polymer. Thus, the μ exponent of eq 7 is close to zero. Conversely, when $\mathbf{l}_j$ gets *across* the branch point the scalar products drop suddenly by about 1 order of magnitude. More precisely, if $\mathbf{l}_i$ is kept on arm 1 (see Chart 1), $\langle \mathbf{l}_i \cdot \mathbf{l}_j \rangle$ decreases by a factor of 3 when $\mathbf{l}_j$ gets past the central branch point and then again by roughly the same factor when it gets past the secondary branch point (i.e., B, C, or D in Chart 1). Afterwards, the scalar products $\langle \mathbf{l}_i \cdot \mathbf{l}_j \rangle$ are very small, equal to that of bonds close to the free ends (see, for instance, the curve of the linear chain with $n = 20$, filled diamonds). The same *quantitative* results are obtained for larger stars, although with a somewhat poorer statistics when the bonds are on different arms. On the other hand, the longer linear chain of Figure 5 (filled triangles, $n = 40$) does not show the downward curvature due to the end effects. Hence, in this case the scalar products are larger than those of the star with $n = 20$ and 40, if the bonds are at the same topological separation but on different arms, even accounting for the range of statistical fluctuations of the larger stars. This means, in conclusion, that the small values of the scalar products for bonds across the branch point are not due to end effects, which anyway are smaller in the star than in the linear chain, as shown in Figure 4 and discussed before. Rather, they indicate that the bond vectors undergo an abrupt loss of correlation, losing memory of the previous direction. This loss of memory among the initial arm directions relieves somewhat the steric interference with the other arms; at the same time, it leaves to each arm the largest possible freedom, thus minimizing the loss of conformational entropy due to the intramolecular expansion. This effect must therefore be more sharp and more complete the larger the number of arms, while being almost absent in lightly branched polymers.

Concluding Remarks

We performed off-lattice Monte Carlo simulations of 12-arm stars to elucidate their local conformation, with particular emphasis on the interatomic distances and the scalar products among bond vectors. The present results support those obtained in paper I in the assumption of a Gaussian distribution for the (perturbed) interatomic distances. The chain expansion turns out to be indeed concentrated in the core region, qualitatively in keeping with other theoretical[4] and simulation[6] results. A somewhat different picture was adopted *a priori* in the scaling analysis of Daoud and Cotton,[26] who modeled the star in terms of spherical shells of blobs. Within this model, the outer blobs show the larger expansion, whereas those closer to the branch point are essentially unperturbed because of the large local concentration of monomers. This picture leads to scaling laws for the overall properties or the density profile apparently in agreement with Monte Carlo simulations;[6] however, only the fully excluded-volume regime could be discerned, whereas the inner unperturbed blobs are missing,[6] in keeping with our results.

A peculiar result obtained in paper I and confirmed by the present simulations is the behavior of the interatomic distances, similar to that shown here in Figure 3, and the ensuing loss of correlation among the arms. In this way, the star can minimize at the same time both the intra- and the interarm repulsion, with not too large an entropic loss. Needless to say, no such loss of correlation is present in the linear chain. The power-law exponents reported here for the local properties (eqs 4−6 and 7) cannot be obtained in the asymptotic limit, unlike those for the global properties. This is due to the finite length of the molecules and the chain portions under investigation, but it might also point to the very inadequacy of simple power laws. On the other hand, even the asymptotic behavior of some overall properties (in particular R_H) is outside the experimentally accessible range. The ν_{ij}^{star} exponent of the interatomic distances within a star arm (see eq 6) is significantly larger than the corresponding exponent for the linear polymer having either the same *total* molecular weight or the same molecular weight *per arm*. Moreover, even within one arm ν_{ij}^{star} changes significantly with the location of the two atoms, since the star expansion is concentrated in the vicinity of the branch point. As to the bond-vector correlation, it is particularly noteworth the strong correlation among the bond vectors belonging to the same arm and close to the branch point and conversely the sharp loss of correlation when they belong to different arms. A rough power-law dependence from topological separation can be found when the two vectors are far from both the free ends and the branch point (see eq 7); although strongly affected by the small number of bonds that can actually be taken into account because of the statistical accuracy that is required, this dependence is consistent with that for the interatomic distances and the radius of gyration.

Acknowledgment. Helpful discussions with Professor Giuseppe Allegra are gratefully acknowledged. This work was financially supported by the Italian Ministry of the University and of the Scientific and Technological Research (MURST, 40%).

References and Notes

(1) Douglas, J. F.; Roovers, J.; Freed, K. F. *Macromolecules* **1990**, *23*, 4168.
(2) See, e.g., Allegra, G.; Ganazzoli, F. *Adv. Chem. Phys.* **1989**, *75*, 265.
(3) Allegra, G.; Colombo, E.; Ganazzoli, F. *Macromolecules* **1993**, *26*, 330.
(4) Miyake, A.; Freed, K. F. *Macromolecules* **1983**, *16*, 1228; **1984**, *17*, 678.
(5) Ganazzoli, F.; Allegra, G.; Colombo, E.; De Vitis, M. *Macromolecules* **1995**, *28*, 1076.
(6) Batoulis, J.; Kremer, K. *Macromolecules* **1989**, *22*, 4277.
(7) Mazur, J.; McCrakin, F. *Macromolecules* **1977**, *10*, 326.
(8) Barrett, A. J.; Tremain, D. L. *Macromolecules* **1987**, *20*, 1687.
(9) Batoulis, J.; Kremer, K. *Europhys. Lett.* **1988**, *7*, 683.
(10) Bruns, W.; Carl, W. *Macromolecules* **1991**, *24*, 209.
(11) Su, S.-J.; Denny, M. S.; Kovac, J. *Macromolecules* **1991**, *24*, 917.
(12) Zifferer, G. *Makromol. Chem., Theory Simul.* **1992**, *1*, 55.
(13) Sikorski, A. *Polymer* **1993**, *34*, 1271.
(14) Grest, G. S. *Macromolecules* **1994**, *27*, 3493.
(15) Metropolis, N.; Rosenbluth, A. W.; Rosenbluth, M. N.; Teller, A. H.; Teller, E. *J. Chem. Phys.* **1953**, *21*, 1087.
(16) Binder, K.; Heermann, D. W. *Monte Carlo Simulations in Statistical Physics*; Springer-Verlag: Berlin, 1992.
(17) Fujita, H. *Polymer Solutions*; Elsevier: Amsterdam, 1990.
(18) LeGuillou, J. C.; Zinn-Justin, J. *Phys. Rev. Lett.* **1977**, *39*, 95; *Phys. Rev. B* **1980**, *21*, 3976.
(19) Weill, G.; des Cloizeaux, J. *J. Phys.* **1979**, *40*, 99.
(20) Nemoto, N.; Makita, Y.; Tsunashima, Y.; Kurata, M. *Macromolecules* **1984**, *17*, 425.
(21) Adam, M.; Delsanti, M. *Macromolecules* **1977**, *10*, 1229.
(22) Zimm, B. H.; Stockmayer, W. H. *J. Chem. Phys.* **1949**, *17*, 1301.
(23) Stockmayer, W. H.; Fixman, M. *Ann. N. Y. Acad. Sci.* **1953**, *57*, 334.
(24) Šolc, K.; Stockmayer, W. H. *J. Chem. Phys.* **1971**, *54*, 2756. Šolc, K. *J. Chem. Phys.* **1971**, *55*, 335.
(25) Batoulis and Kremer[6] get $\mu = 1.15$ for the linear chain, which is too large according to the comments made after eq 7. However, there is a possible error in the abscissa of their Figures 12 and 13, which should read $i - j + 1$ and not $i - j$, since they get $\langle \mathbf{l}_i \cdot \mathbf{l}_j \rangle = 1$ for a unit value of the abscissa. This can be true only if $i = j$ and not if $i = j + 1$, as they state. With this change in the abscissa, they should get a smaller μ value, perhaps in the acceptable range $\mu < 1$.
(26) Daoud, M.; Cotton, J. P. *J. Phys.* **1982**, *43*, 531.

MA9508820